LETTER Communicated by Laurence Abbott

Computing the Optimally Fitted Spike Train for a Synapse

Thomas Natschläger
Wolfgang Maass
Institute for Theoretical Computer Science, Technische Universität Graz, Graz, Austria

Experimental data have shown that synapses are heterogeneous: different synapses respond with different sequences of amplitudes of postsynaptic responses to the same spike train. Neither the role of synaptic dynamics itself nor the role of the heterogeneity of synaptic dynamics for computations in neural circuits is well understood. We present in this article two computational methods that make it feasible to compute for a given synapse with known synaptic parameters the spike train that is optimally fitted to the synapse in a certain sense. With the help of these methods, one can compute, for example, the temporal pattern of a spike train (with a given number of spikes) that produces the largest sum of postsynaptic responses for a specific synapse. Several other applications are also discussed. To our surprise, we find that most of these optimally fitted spike trains match common firing patterns of specific types of neurons that are discussed in the literature. Hence, our analysis provides a possible functional explanation for the experimentally observed regularity in the combination of specific types of synapses with specific types of neurons in neural circuits.

1 Introduction

A large number of experimental studies have shown that biological synapses have an inherent dynamics, which controls how the pattern of amplitudes of postsynaptic responses depends on the temporal pattern of the incoming spike train (Katz, 1966; Magleby, 1987; Markram & Tsodyks, 1996; Thomson, 1997; Varela et al., 1997; Dobrunz & Stevens, 1999). Various quantitative models have been proposed (Varela et al., 1997; Abbott, Varela, Sen, & Nelson, 1997; Markram, Wang, & Tsodyks, 1998) involving a small number of hidden parameters, which allow us to predict the response of a given synapse to a given spike train once proper values for these hidden synaptic parameters have been found. The analysis of this article is based on the model of Markram et al. (1998), where three parameters U, F, D control the dynamics of a synapse. A fourth parameter A, which corresponds to the synaptic "weight" in static synapse models, scales the absolute sizes of the postsynaptic responses. The resulting model predicts the amplitude $A_m = A \cdot u_m \cdot R_m$ of the postsynaptic response to the $(m+1)$th spike in a

 © 2001 Massachusetts Institute of Technology

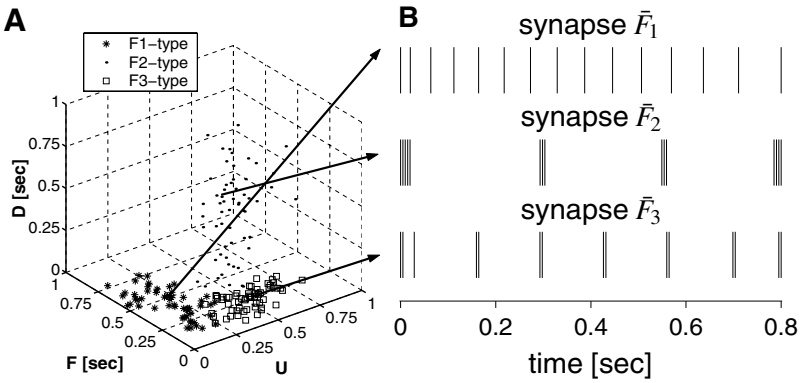

Figure 1: (A) Synaptic heterogeneity. Shown is the distribution of values of the parameters U, F, D for inhibitory synapses investigated in Gupta et al. (2000), which can be grouped into three major classes: facilitating (F1), depressing (F2), and recovering (F3). (B) Spike trains that maximize the sum of postsynaptic responses for three given synapses ($T = 0.8$ sec, $n+1 = 15$ spikes). The parameters for synapses $\bar{F}_1$, $\bar{F}_2$, and $\bar{F}_3$ are the mean values for the synapse types F1, F2, and F3 reported in Gupta et al. (2000) (see Figure 2 for numerical values).

spike train with interspike intervals (ISI's) $\Delta_0, \Delta_1, \ldots, \Delta_{m-1}$, through the equations[1]

$$u_{k+1} = U + u_k(1 - U)\exp(-\Delta_k/F)$$
$$R_{k+1} = 1 + (R_k - u_k R_k - 1)\exp(-\Delta_k/D), \tag{1.1}$$

which involve two hidden dynamic variables $u \in [0, 1]$ and $R \in [0, 1]$ with the initial conditions $u_0 = U$ and $R_0 = 1$ for the first spike. These dynamic variables evolve in dependence of the synaptic parameters U, F, D and the interspike intervals of the incoming spike train. It should be noted that this deterministic model predicts the cumulative response of a population of stochastic release sites that make up a synaptic connection. Gupta, Wang, and Markram (2000) reported that the synaptic parameters U, F, D are quite heterogeneous, even within a single neural circuit (see Figure 1A). Note that the time constants D and F are in the range of a few hundred ms. The synapses investigated in Gupta et al. (2000) can be grouped into three major classes: facilitating (F1), depressing (F2), and recovering (F3).

In this article, we address the question which temporal pattern of a spike train is optimally fitted to a given synapse characterized by the three param-

[1] To be precise, the term $u_k R_k$ in eq. 1.1 was erroneously replaced by $u_{k+1} R_k$ in the corresponding equation 2 of Markram et al. (1998). The model that they actually fitted to their data is the model considered in this article.

eters U, F, D in a certain sense. One possible choice is to look for the temporal pattern of a spike train that produces the largest sum $\sum_{k=0}^{n} A \cdot u_k \cdot R_k$ of postsynaptic responses. In the original formulation of the model (Markram et al., 1998) $A_m = A \cdot u_m \cdot R_m$ describes the amplitude of the excitatory postsynaptic current (or excitatory postsynaptic potential) triggered by the $(m+1)$th spike in a spike train. Hence, the larger the sum $\sum_{k=0}^{n} A \cdot u_k \cdot R_k$ is, the larger is the net effect of the synapse on its target neuron. Another interesting optimality criterion is the maximal integral of synaptic current. Note that in the case where the dendritic integration is approximately linear, the two optimality criteria maximal integral of synaptic current and maximal sum $\sum_{k=0}^{n} A \cdot u_k \cdot R_k$ are equivalent.[2] We would like to stress that the computational methods we present are not restricted to any particular choice of the optimality criterion. For example, one can use them also to compute the spike train that produces the largest peak of the postsynaptic membrane voltage. We defer the discussion of such alternative optimality criteria to section 4 and focus in sections 2 and 3 on the question of which temporal pattern of a spike train produces the largest sum $\sum_{k=0}^{n} A \cdot u_k \cdot R_k$ of postsynaptic responses (or, equivalently, the largest integral of postsynaptic current).

As we will discuss in section 2, there exists an algorithm to compute for a given synapse the spike train that produces the largest sum $\sum_{k=0}^{n} A \cdot u_k \cdot R_k$ exactly. Hence, such an algorithm maps each point (a given synapse) of the parameter space (three dimensions U, F, D in our case) onto a point (a particular spike train) in the space of spike trains (see Figure 1).

More precisely, we fix a time interval T, a minimum value $\Delta_{\min}$ for interspike intervals (ISIs), a natural number n, and synaptic parameters U, F, D. We then look for that spike train with $n+1$ spikes during T and ISIs $\geq \Delta_{\min}$ that maximizes $\sum_{k=0}^{n} A \cdot u_k \cdot R_k$. Hence we seek a solution—that is, a sequence of ISIs $\Delta_0, \Delta_1, \ldots, \Delta_{n-1}$—to the optimization problem

$$\begin{aligned} &\text{maximize} \sum_{k=0}^{n} A \cdot u_k \cdot R_k \\ &\text{under} \sum_{k=0}^{n-1} \Delta_k \leq T \text{ and } \Delta_{\min} \leq \Delta_k, \quad k = 0, \ldots, n-1. \end{aligned} \tag{1.2}$$

In section 2, we present an algorithmic approach based on dynamic programming (DP) that is guaranteed to find the optimal solution of the optimization problem, equation 1.2 (up to discretization errors), and exhibit for six major types of synapses temporal patterns of spike trains that are

[2] In the linear case, the synaptic current $I_{syn}(t)$ can be modeled as $I_{syn}(t) = A \sum_{k=0}^{n} u_k R_k \varepsilon(t - t_k)$, with $\varepsilon(t) = \frac{t}{\tau_s} \exp(\frac{t}{\tau_s} + 1)$ (τ_s synaptic time constant). Hence, $\int I_{syn}(t)\, dt = A \sum_{k=0}^{n} u_k R_k \int \varepsilon(t - t_k)\, dt$, where $\int \varepsilon(t - t_k)\, dt$ is constant if the integration time window is large enough ($> 5 \cdot \tau_s$).

optimally fitted to these synapses. In section 3 we present a faster heuristic method for computing optimally fitted spike trains and apply it to analyze how their temporal pattern depends on the number $n+1$ of allowed spikes during time interval T, that is, on the firing rate. Furthermore, we analyze in section 3 how changes in the synaptic parameters U, F, D and the spiking history affect the temporal pattern of the optimally fitted spike train. In section 4 we discuss the application of the presented computational methods for other optimality criteria than the maximal sum of postsynaptic responses.

2 Computing Optimal Spike Trains for Common Types of Synapses

2.1 Dynamic Programming. For $T = 1000$ ms and $n = 10$, there are about 2^{100} spike trains among which one wants to find the optimally fitted one. We show that a computationally feasible solution to this complex optimization problem can be achieved via dynamic programming. We refer to Bertsekas (1995) for the mathematical background of this technique, which also underlies the computation of optimal policies in reinforcement learning. We consider the discrete-time dynamic system described by the equation

$$x_0 = \langle U, 1, 0\rangle \quad \text{and} \quad x_{k+1} = f(x_k, a_k) \quad \text{for } k = 0, 1, \ldots, n-1, \tag{2.1}$$

where x_k describes the state of the system at step k and a_k is the "control" or "action" taken at step k. In our case, x_k is the triple $\langle u_k, R_k, t_k\rangle$ consisting of the values of the dynamic variables u and R used to calculate the amplitude $A \cdot u_k \cdot R_k$ of the $(k+1)$th postsynaptic response and the time t_k of the arrival of the $(k+1)$th spike at the synapse. The "action" a_k is the length $\Delta_k \in [\Delta_{\min}, T - t_k]$ of the $(k+1)$th ISI in the spike train that we construct, where $\Delta_{\min}$ is the smallest possible size of an ISI (we have set $\Delta_{\min} = 5$ ms in our computations). As the function f in equation 2.1, we take the function that maps $\langle u_k, R_k, t_k\rangle$ and Δ_k via equation 1.1 on $\langle u_{k+1}, R_{k+1}, t_{k+1}\rangle$ for $t_{k+1} = t_k + \Delta_k$. The "reward" for the $(k+1)$th spike is $A \cdot u_k \cdot R_k$, that is, the amplitude of the postsynaptic response for the $(k+1)$th spike. Hence, maximizing the total reward $J(x_0) = \sum_{k=0}^{n} A \cdot u_k \cdot R_k$ is equivalent to solving the maximization problem, equation 1.2. The maximal possible value of $J_0(x_0)$ can be computed exactly using the equations

$$\begin{aligned} J_n(x_n) &= A \cdot u_n \cdot R_n \\ J_k(x_k) &= \max_{\Delta \in [\Delta_{\min}, T - t_k]} (A \cdot u_k \cdot R_k + J_{k+1}(f(x_k, \Delta))) \end{aligned} \tag{2.2}$$

backward from $k = n-1$ to $k = 0$. Thus, the optimal sequence $a_0, \ldots, a_{n-1}$ of "actions" is the sequence $\Delta_0, \ldots, \Delta_{n-1}$ of ISIs that achieves the maximal possible value of $\sum_{k=0}^{n} A \cdot u_k \cdot R_k$. Note that the evaluation of $J_k(x_k)$ for a

single value of x_k requires the evaluation of $J_{k+1}(x_{k+1})$ for many different values of x_{k+1}.

When one solves equation 2.2 on a computer, one has to replace the continuous-state variable x_k by a discrete variable $\tilde{x}_k$ and round $x_{k+1} := f(\tilde{x}_k, \Delta)$ to the nearest value of the corresponding discrete variable $\tilde{x}_{k+1}$. This means that instead of applying equation 1.1, one updates the values of the hidden dynamic variables u and R and the auxiliary variable t_k by the equations

$$\begin{aligned}\tilde{u}_{k+1} &= [U + \tilde{u}_k(1 - U)\exp(-\Delta_k/F)]_\delta \\ \tilde{R}_{k+1} &= [1 + (\tilde{R}_k - \tilde{u}_k \cdot \tilde{R}_k - 1)\exp(-\Delta_k/D)]_\delta \\ \tilde{t}_{k+1} &= [\tilde{t}_k + \Delta_k]_{\Delta t},\end{aligned} \tag{2.3}$$

where $[z]_\epsilon$ denotes the nearest discrete value of z with discretization interval ϵ. Computer simulations (see the appendix) show that for the values of T and n that are considered in this article, it suffices to choose a discretization where $\tilde{u}_k \in \{0, \delta, 2\delta, \ldots, 1\}$, $\tilde{R}_k \in \{0, \delta, 2\delta, \ldots, 1\}$ with $\delta = 1/50$ and $\tilde{t}_k \in \{0, \Delta t, \ldots, T\}$ with $\Delta t = 1$ ms. For this choice, the trajectory in the resulting discrete dynamic system, equation 2.3, approximates the trajectory in the continuous system, equation 1.1, very well. Therefore, we have based the computations of optimal spike trains for major synapse types that are discussed in the next paragraph on equation 2.3, with $\delta = 1/50$ and $\Delta t = 1$ ms.

2.2 Results. We have applied the dynamic programming approach to six major types of synapses reported in Gupta et al. (2000) and Markram et al. (1998). The results are summarized in Figure 2.

We refer informally to the temporal pattern of $n + 1$ spikes that maximizes the response of a particular synapse as the "key to this synapse." It is shown in Figure 3A that the "keys" for the inhibitory synapses ($\bar{F}_1$, $\bar{F}_2$, and $\bar{F}_3$) are rather specific in the sense that they exhibit a substantially smaller postsynaptic response on any other of the major types of inhibitory synapses reported in Gupta et al. (2000).

A noteworthy—and possibly interesting—aspect of the "keys" shown in Figure 2 (and in Figures 4 and 5) is that they correspond to common firing patterns (accommodating, nonaccommodating, stuttering, bursting, and regular firing) of neocortical interneurons (reported under controlled conditions in vitro; Gupta et al., 2000, Fig. 5). For example, the optimal spike trains for synapses $\bar{F}_2$ and $\bar{F}_3$ are similar to the output of a stuttering cell. In the same manner, one can classify the optimal spike trains for synapses $\bar{F}_1$ and E_3 as accommodating (see also Figure 4).

Another interesting effect arises by comparing the optimal values of the sum $\sum_{k=0}^{n} u_k \cdot R_k$ for synapses $\bar{F}_1$, $\bar{F}_2$, and $\bar{F}_3$ (see Figure 3B) with the maximal values of $\sum_{k=0}^{n} A \cdot u_k \cdot R_k$ (see Figure 3C), where we have set A equal to the value of $G_{\max}$ reported in Gupta et al. (2000, Table 1). Whereas the values of

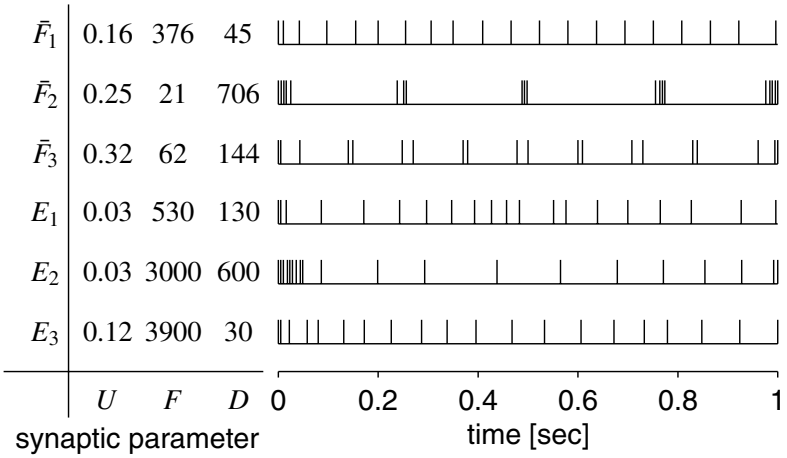

Figure 2: Spike trains that maximize the sum of postsynaptic responses for six common types of synapses ($T = 1$ sec, 20 spikes). The parameters (D and F in ms) for synapses $\bar{F}_1$, $\bar{F}_2$, and $\bar{F}_3$ are the mean values for the synapse types F1, F2, and F3 reported in Gupta et al. (2000, Table 1). Parameters for synapses E_1, E_2, and E_3 are taken from Markram et al. (1998, Fig. 3).

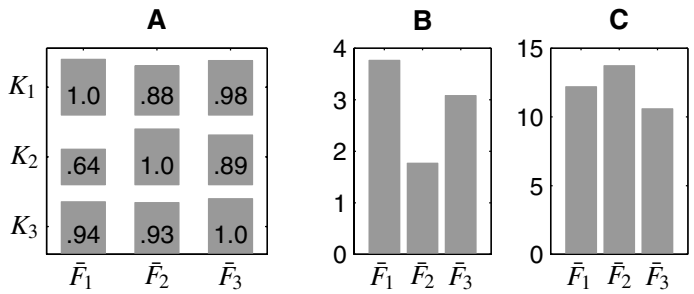

Figure 3: (A) Specificity of optimal spike trains. The optimal spike trains for synapses $\bar{F}_1$, $\bar{F}_2$, and $\bar{F}_3$ (denoted by K_1, K_2, and K_3, respectively) obtained for $T = 1$ sec and 10 spikes (see the bottom traces in Figure 4) are tested on the other two types of synapses. Plotted is the value of the sum of the postsynaptic response of each synapse $\bar{F}_i$ to spike train K_j with $j \neq i$ in relation to its response to K_i. The plotted values are normalized to have value 1 for the pairs $\langle K_i, \bar{F}_i \rangle$, $i = 1, 2, 3$. (B) Absolute values of the sums $\sum_{k=0}^{n} u_k \cdot R_k$ if the spike train K_i is applied to synapse $\bar{F}_i$, $i = 1, 2, 3$. (C) Same as B except that the value of $A \cdot \sum_{k=0}^{n} u_k \cdot R_k$ is plotted. For A we used the value of $G_{\max}$ (in nS) reported in Gupta et al. (2000, Table 1). The quotient max/min is 1.3 compared to 2.13 in B.

$G_{\max}$ vary strongly among different synapse types, the resulting maximal response of a synapse to its proper "key" is almost the same for each synapse. Hence, one may speculate that the system is designed in such a way that each synapse should have an equal influence on the postsynaptic neuron when it receives its optimal spike train. This effect is most evident for a spiking frequency $(n+1)/T$ of 10 Hz and vanishes for frequencies above 20 Hz.

3 Exploring the Parameter Space

3.1 Sequential Quadratic Programming. The numerical approach for approximately computing optimal spike trains that was used in section 2 is sufficiently fast that an average PC can carry out any of the computations whose results were reported in Figure 2 within a few hours. To be able to address computationally more expensive issues, we used a nonlinear optimization algorithm known as sequential quadratic programming (SQP),[3] which is the state-of-the-art approach for heuristically solving constrained optimization problems such as equation 1.2. (See Powell, 1983, for the mathematical background of this technique.) Applying this algorithm requires calculating the partial derivatives $\frac{\delta J}{\delta \Delta_i}$ of the objective function $J(\Delta_0, \ldots, \Delta_{n-1}) = \sum_{k=0}^{n} u_k \cdot R_k$ with respect to Δ_i for $i = 0, \ldots, n-1$. The calculations of these partial derivatives are found in the appendix. To compute an optimal spike train, we perform 100 runs of the SQP algorithm with different random initializations and select the result with the highest value of $\sum_{k=0}^{n} u_k R_k$.

Unfortunately, the SQP algorithm is not guaranteed to find the optimal spike train, even if the numerical precision is sufficiently high, since it could in principle get stuck in local extrema. However, in all our tests, SQP has produced within a few minutes of computation time a solution that is very close to the spike train computed by the more rigorous dynamic programming approach (for comparison, see the spike trains marked by a gray background in Figure 4). This observation suggests that SQP tends to find near to optimal solutions to the optimization problem, equation 1.2.[4]

3.2 Optimal Spike Trains for Different Firing Rates. First we used SQP to explore the effect of the spike frequency $(n+1)/T$ on the temporal pattern of the optimal spike train. For the synapses $\bar{F}_1$, $\bar{F}_2$, and $\bar{F}_3$, we computed the optimal spike trains for frequencies ranging from 10 Hz to 35 Hz. The

[3] We used the implementation (function `constr`) contained in the MATLAB Optimization Toolbox (see http://www.mathworks.com/products/optimization/).

[4] The deviations between the solutions of SQP and DP also originate in part from the fact that SQP is applied to the continuous model, equation 1.1, whereas DP has to be applied to the discrete model, equation 2.3. A useful consequence is that if the DP solution is used as initialization for the SQP algorithm, one can sometimes improve the DP solution slightly.

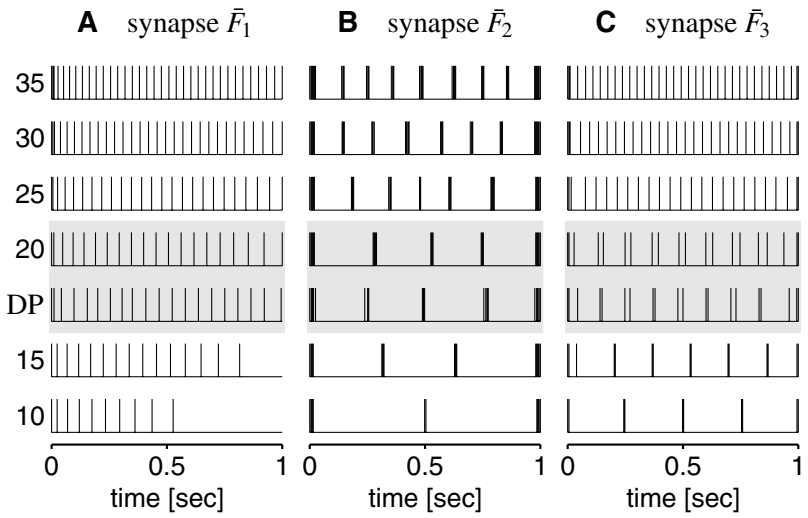

Figure 4: Dependence of the optimal spike train on the spike frequency $(n+1)/T$ ($T = 1$ sec, $n + 1 = 10, \ldots, 35$). For each of the synapses $\bar{F}_1$, $\bar{F}_2$, and $\bar{F}_3$, the optimal spike train is plotted for different frequencies (from 10 Hz to 35 Hz). To compare the solutions of SQP and DP, we also show as an example the solution for 20 Hz obtained by DP (spike trains labeled DP), which occurred already in Figure 2.

results are summarized in Figure 4. For synapses $\bar{F}_1$ and $\bar{F}_2$, the characteristic spike pattern ($\bar{F}_1$ ... accommodating, $\bar{F}_2$ ... stuttering) is the same for all frequencies. In contrast, the optimal spike train for synapse $\bar{F}_3$ has a phase transition from stuttering to nonaccommodating at about 20 Hz.

3.3 The Impact of Individual Synaptic Parameters. We now address the question how the optimal spike train depends on the individual synaptic parameters U, F, and D. Since the parameters D and F of synapse $\bar{F}_3$ lie between the $D-$ and $F-$values of synapses $\bar{F}_1$ and $\bar{F}_2$, it is not surprising that the most interesting effects occur when one changes U, F, D in the vicinity of the parameters of synapse $\bar{F}_3$. The results are summarized in Figure 5, which shows that the optimal spike train moves through the same temporal patterns (even in the same order), no matter which of the three parameters is varied. Another interesting observation is that the sum of postsynaptic responses (gray horizontal bars in Figure 5) depends primarily on the temporal pattern of the optimal spike train and not that much on the actual values of U, F, D for which this pattern is optimal.

We have marked in Figure 5 the range of parameters for synapses of type F3 reported in Gupta et al. (2000, Table 1) with a black bar (the pa-

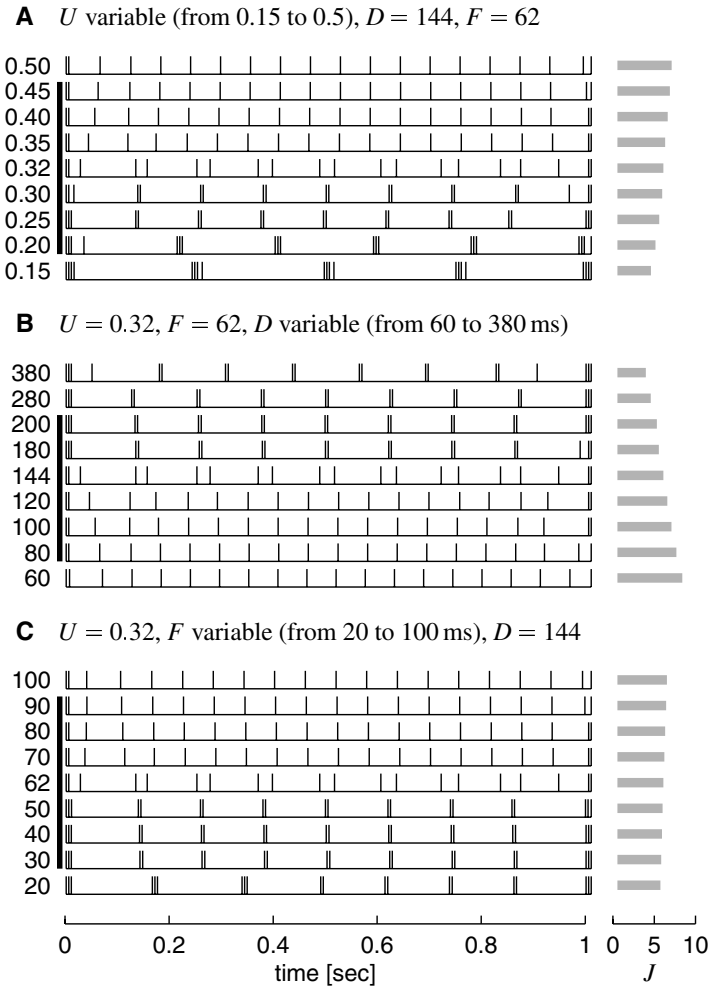

Figure 5: Dependence of the optimal spike train on the synaptic parameters U, F, D. Each panel shows how the optimal spike train changes if one parameter is varied. The other two parameters are set to the value corresponding to synapse $\bar{F}_3$ (see Figure 2). The black bar to the left marks the range of values (mean $\pm$std) reported in Gupta et al. (2000) for the parameter that varies. To the right of each spike train we plotted the corresponding value of $J = \sum_{k=0}^{n} u_k R_k$ (gray bars).

rameters of synapse $\bar{F}_3$ are the reported mean values for synapses of type F3). Within this parameter range, we find stuttering and nonaccommodating spike patterns, with a phase transition right in the middle. We also

calculated the optimal spike trains for the range of parameters U, F, D for synapses of the types F1 and F2 reported in Gupta et al. (2000, Table 1) (results not shown in this article). We found that the temporal pattern of the optimal spike train for the variations within the class of F1 (F2) synapses is always of class accommodating (stuttering).

3.4 Influence of the Spiking History. So far we had implicitly assumed—through the initial conditions $u_0 = U$ and $R_0 = 1$—that the input spike train follows a long period of complete presynaptic inactivity. However, initial conditions other than $u_0 = U$ and $R_0 = 1$ can account for an arbitrary spiking history of the synapse under consideration. This is due to the fact that an arbitrary spike train with $(m + 1)$ spikes and ISIs $\Delta_0, \Delta_1, \ldots, \Delta_{m-1}$ yields certain values u_m and R_m of the hidden dynamic variables u and R. Thus, using these values as initial values u_0 and R_0 in our computation of an optimal fitted spike train, we effectively compute the optimally fitted spike train after the synapse had previously received a spike train with ISIs $\Delta_0, \Delta_1, \ldots, \Delta_{m-1}$.[5]

Figure 6 shows the impact of different initial conditions u_0 and R_0 on the optimally fitted spike train for synapse $\bar{F}_3$. The basic firing pattern (nonaccommodating) does not change, but the onset of firing is delayed. The amount of delay increases with the level of depression (low R_0) and increasing u_0 (fraction of resources used per spike). This also holds for the synapses $\bar{F}_1$ and $\bar{F}_2$ (results not shown). Note that the resulting optimal spike trains for $u_0, R_0 < 1$ match another family of firing patterns: delayed discharge (see column 3 of Figure 5 in Gupta et al., 2000).

4 Other Optimality Criteria

In this section, we discuss the application of the computational methods we have introduced to the computation of spike trains that are optimally fitted to a given synapse in a sense other than that discussed in the previous sections (largest sum $\sum_{k=0}^{n} A \cdot u_k \cdot R_k$). A list of alternative criteria with respect to which a spike train can be defined as optimal for a given synapse may include the following:

A. Maximal amplitude of a certain (e.g., the last ($i = n$)), postsynaptic response:

$$\text{maximize } u_i \cdot R_i \tag{4.1}$$

B. Maximal amplitude of the largest postsynaptic response:

$$\text{maximize } \max_{0 \le k \le n} \{u_k \cdot R_k\} \tag{4.2}$$

[5] Due to this notation, the first spike of each optimally fitted spike train should be interpreted as the $(m+1)$ spike of the spiking history described by the ISIs $\Delta_0, \Delta_1, \ldots, \Delta_{m-1}$.

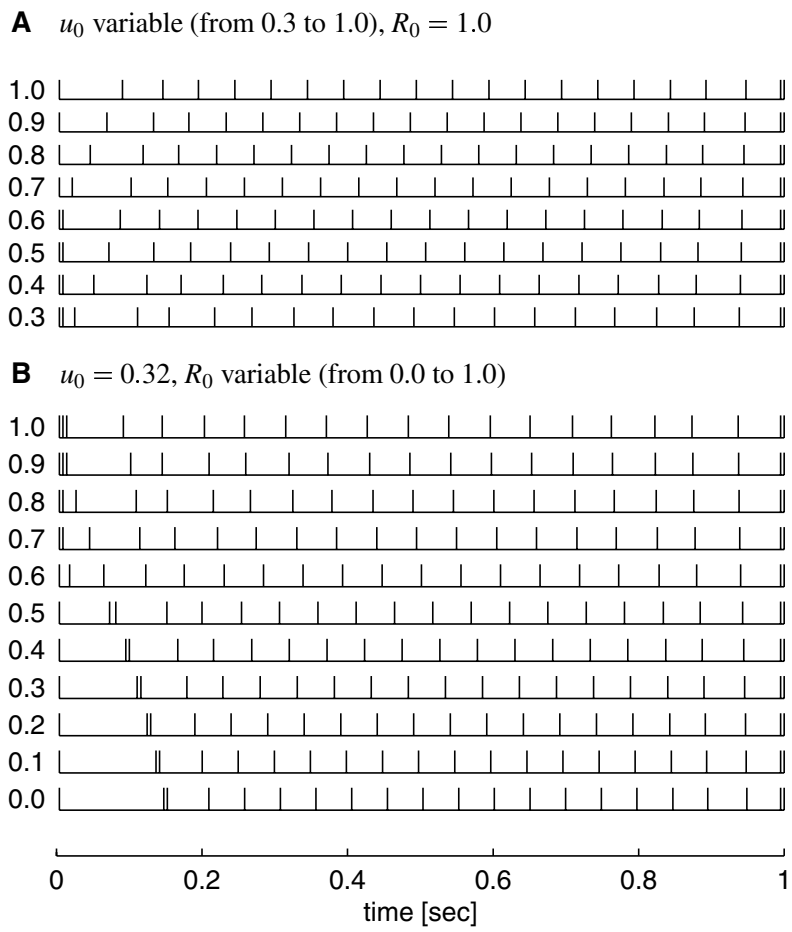

Figure 6: Dependence of the optimal spike train of synapse $\bar{F}_3$ (see Figure 2 for parameter values) on the initial values u_0 and R_0. Each panel shows how the optimal spike train changes if one value is varied. The other value holds constant.

C. Maximal peak of postsynaptic membrane potential V(t)[6]:

$$\text{maximize} \max_{0 \le t \le T} \{V(t)\} \tag{4.3}$$

[6] The membrane voltage $V(t)$ can be modeled by $\tau_m \frac{dV(t)}{dt} = -V(t) + I_{syn}(t)$, where $\tau_m = 50$ ms is the membrane time constant and $I_{syn}(t) = A \cdot \sum_{k=0}^{n} u_k \cdot R_k \cdot \varepsilon(t - t_k)$ is the synaptic current, with $\varepsilon(t) = \frac{t}{\tau_s} e^{(-t/\tau_s + 1)}$ and $\tau_s = 2$ ms. t_k denotes the time of the $(k+1)$th spike in the input spike train.

D. Maximal specificity of several spike trains among several synapses:

$$\text{maximize} \sum_{1\le i\le l} c_{ii} - \sum_{1\le i\ne j\le l} c_{ij} \tag{4.4}$$

where c_{ij} are the values of a specificity matrix $C = [c_{ij}]_{1\le i,j\le l}$, an example of which is shown in Figure 3. Note that here l spike trains (one for each synapse) are computed simultaneously.

As before these criteria are considered under the constraints $\sum_{k=0}^{n-1} \Delta_k \le T$ and $\Delta_{\min} \le \Delta_k, k = 0, \ldots, n-1$.

In principle, the DP approach would allow computing the exact solution for all of the corresponding constrained optimization problems. However, one has to cope with the problem that the dimension of the state variables x_k (see equation 2.1) has to be enlarged to incorporate additional information (e.g., the current maximum or the current membrane potential). This has the fatal consequence that it is impossible to run the DP algorithm on an average PC.

Fortunately, it is rather straightforward to adapt the SQP approach to these other optimization problems. Note, however, that for criteria B and C, an analytical form of the partial derivatives $\frac{\delta J}{\delta \Delta_i}$, $i = 0, \ldots, n-1$ of the corresponding objective function $J(\Delta_0, \ldots, \Delta_{n-1})$ in general cannot be obtained. But the partial derivatives $\frac{\delta J}{\delta \Delta_i}$ are piecewise continuous and can be approximated numerically (by a finite difference quotient) quite well.

The optimally fitted spike trains for synapses $\bar{F}_1$, $\bar{F}_2$, and $\bar{F}_3$ for each of the above optimality criteria obtained with the SQP algorithm are shown in Figure 7.

Figure 7: *Facing page*. Optimally fitted spike trains for synapses $\bar{F}_1$, $\bar{F}_2$, and $\bar{F}_3$ for the four other optimality criteria. (A1) Spike trains for $T = 0.5$ sec and 10 spikes, which maximize the amplitude of the last synaptic response. The amplitude $u_k \cdot R_k$ is represented by the height of the $(k+1)$th vertical line. (A2) Shows (for the same optimization criterion) the dependence of the maximally achievable amplitude of the synaptic response for the last spike on the number of spikes in the spike train. (B1) Same as A1 but spike trains maximize the amplitude of the largest synaptic response. (B2) Same as A2, but for this different optimization criterion. Amplitude of the largest synaptic response for different numbers of spikes. (C1) Same as A1, but spike trains maximize the peak of the postsynaptic membrane potential (for a given number of spikes). (C2) Postsynaptic potential $V(t)$ corresponding to the optimal spike trains shown in C1 (vertical scale depends on actual electrophysiological parameters). (D1) The three spike trains shown (K1, K2, and K3) maximize the specificity (see equation 4.4) among the synapses $\bar{F}_1$, $\bar{F}_2$, and $\bar{F}_3$. (D2) Specificity matrix for the spike trains shown in D1. For details, see equation 4.4 and Figure 3.

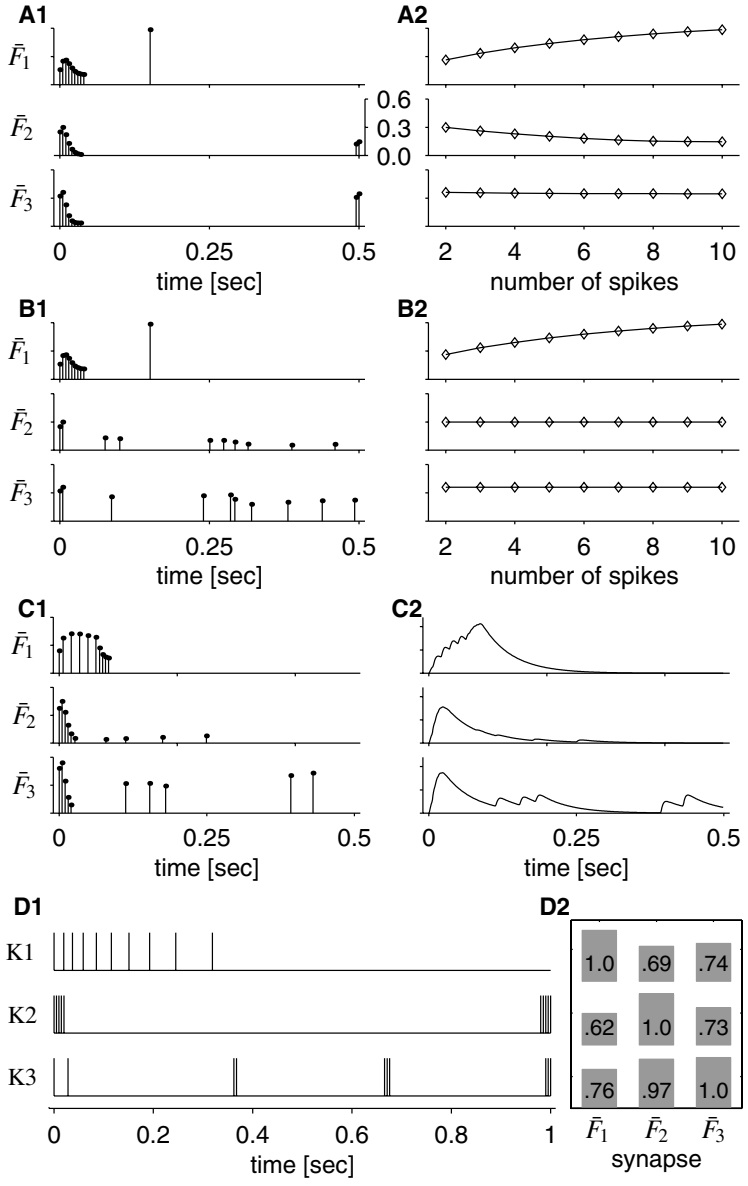

In the following, we provide some remarks regarding the results:

A1 and A2. Note that the resulting optimal temporal pattern of the spike trains happens to be similar to the protocol used for determining synapse types in Gupta et al. (2000).

B1 and B2. For synapse $\bar{F}_1$, the last synaptic response also has the largest amplitude. For $\bar{F}_2$ and $\bar{F}_3$, the second spike always triggers the largest synaptic response.

C1 and C2. For synapse $\bar{F}_1$, a burst with frequency lower than $1/\Delta_{\min}$ yields the largest peak in postsynaptic potential. Note that for $\bar{F}_2$ and $\bar{F}_3$, the spikes occurring after the peak in the membrane voltage are arbitrarily positioned in time.

D1 and D2. A comparison of the spike trains shown in Figure 7, D1, and Figure 2 shows that the qualitative nature of the spike trains is very similar and that the specificity shown in Figure 3 is very similar to the optimal specificity shown in Figure 7, D2.

5 Discussion

We have presented two complementary computational approaches for computing spike trains that optimize a given response criterion for a given synapse. One of these methods is based on dynamic programming (similar as in reinforcement learning), the other on sequential quadratic programming.

Recent studies (Gupta et al., 2000) indicate that GABAergic synapses in neocortical layers II to IV belong to one of three major classes, called F1-, F2-, and F3-type synapses, respectively. It turns out that the spike trains that maximize the response of these types of synapses are well-known firing patterns (accommodating, nonaccommodating, stuttering, bursting, and regular firing) of specific neuron types. For F1- and F3-type synapses, the optimal spike train agrees with the most often found firing pattern of presynaptic neurons reported in Gupta et al. (2000), whereas for F2-type synapses, there is no such agreement.

Note, however, that the firing pattern of interneurons reported in Gupta et al. (2000) were obtained in cortical interneurons in vitro following injection of current steps and may or may not represent how these neurons discharge in vitro. There are also many in vivo studies of discharge characteristics of classes of cortical neurons (Steriade, Timofeev, Dürmüller, & Grenier, 1998; Gray & McCormick, 1996). Steriade et al. (1998) report a class of neurons—so-called fast-rhythmic bursting (FRB) neurons—with discharge patterns (in response to current injection) that have similar properties as the optimal spike train for synapse $\bar{F}_2$ shown in Figure 2: rhythmic bursts with a very high intraburst frequency. If the current injection into FRB neurons is increased, the number of bursts, as well as the number of spikes per burst, increases as well. This is also characteristic for the optimal spike train for synapse $\bar{F}_2$ (see Figure 4) if the spike frequency $(n+1)/T$ is increased. Hence, a synapse of the F2-type would filter the spike train in such a way that FRB neurons have the maximal possible impact on a target neuron over a broad range of firing frequencies. On the other hand Gray and McCormick (1996)

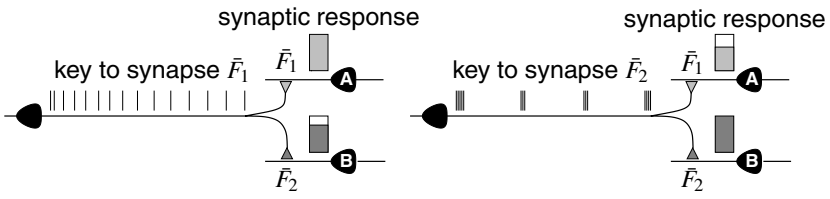

Figure 8: Preferential addressing of postsynaptic targets. Due to the specificity of the optimal spike train of a synapse, a presynaptic neuron may address (i.e., evoke stronger response at) either neuron A or B, depending on the temporal pattern of the spike train (with the same frequency $f = (n+1)/T$) it produces ($T = 0.8$ sec and $(n+1) = 15$ spikes in this example).

report a class of neurons called "chattering cells" that display discharge of repeated (80 Hz) brief (5 spikes) high-frequency (800 Hz) bursts. We have not yet seen such spiking patterns in our studies (even if we use $\Delta_{\min} = 1$ ms). This is probably due to the fact that the synapse model we used (Markram et al., 1998) was derived and validated for synapses of neurons that show much lower firing frequencies. These observations show that our new computational techniques provide tools for analyzing the possible functional role of the specific combinations of synapse types and neuron types that was recently found in Gupta et al. (2000).

Another noteworthy aspect of the optimal spike trains is their specificity for a given synapse (see Figure 3); suitable temporal firing patterns activate preferentially specific types of synapses. One may speculate that due to this feature, a neuron can activate a particular subpopulation of its target neurons by generating a series of action potentials (of a fixed mean frequency) with a suitable temporal pattern (see Figure 8 for an illustration). Recent experiments (Wang & McCormick, 1993; Brumberg, Nowak, and McCormick, 2000) show that neuromodulators can control the firing mode of cortical neurons. Wang and McCormick (1993) show that bursting neurons may switch to regular firing if norepinephine is applied. Together with the specificity of synapses to certain temporal patterns, these findings point to one possible mechanism how neuromodulators can change the effective connectivity of a neural circuit. Furthermore, we have shown in section 4 (see Figure 7, D2) that for the types of synapses discussed in Gupta et al. (2000), spike trains that maximize the response of any single one of these synapses have already close to the optimal specificity.

Our analysis provides the platform for a deeper understanding of the specific role of different synaptic parameters, because with the help of the computational techniques that we have introduced, one can now see directly how the temporal structure of the optimal spike train for a synapse depends on the individual synaptic parameters. We believe that this inverse analysis is essential for understanding the computational role of neural circuits.

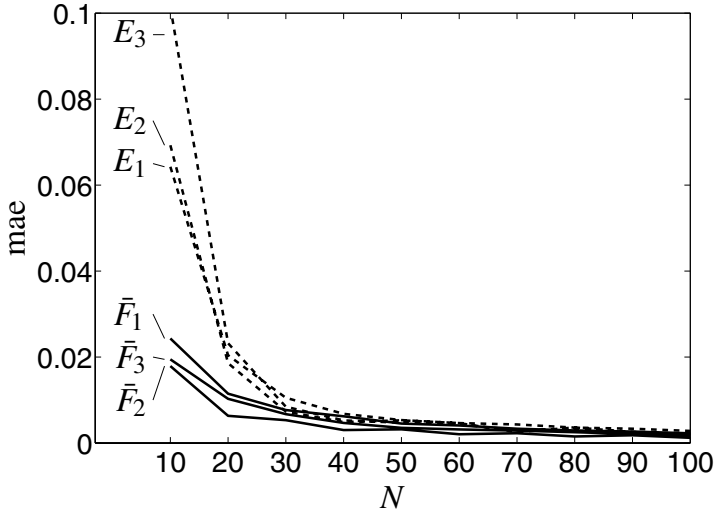

Figure 9: Impact of discretization for dynamic programming. For different synapses (see Figure 2 for parameters), we plotted the average mean absolute error (mae) between the trajectory of the discrete and the continuous model for various levels of discretization intervals $\delta = 1/N$ (for details, see the text).

Appendix A: Impact of Discretization for Dynamic Programming

To assess the influence of the degree of discretization on the trajectory of the synaptic model, we measured the mean absolute error $\frac{1}{n+1}\sum_{k=0}^{n}|u_k R_k - \tilde{u}_k \tilde{R}_k|$ between the trajectory of the discrete model, equation 3.3, and the continuous model, equation 1.1. For each synapse type, we calculated the mean absolute error as an average over 1000 Poisson spike trains consisting of 20 spikes and a mean frequency of 20 Hz. The calculations were performed for various discretization intervals $\delta = 1/N$. The results are summarized in Figure 9. We used $N = 50$ for the computations in section 3.

Appendix B: Partial Derivatives of the Objective Function for Use with SQP

In this section we give a calculation of the partial derivatives $\frac{\delta J}{\delta \Delta_i}$, $i = 0, \ldots, n-1$ of the objective function $J(\Delta_0, \ldots, \Delta_{n-1}) = \sum_{k=0}^{n} A u_k R_k$. Obviously one has to calculate the derivatives $\frac{\delta u_k R_k}{\delta \Delta_i}$ for $k = 0, \ldots, n$ and $i = 0, \ldots, n-1$. For $k \leq i$, one has $\frac{\delta u_k R_k}{\delta \Delta_i} = 0$ since Δ_i influences only

u_k and R_k if $k > i$. In that case ($k > i$) one gets

$$\begin{aligned}\frac{\delta\, u_k R_k}{\delta\, \Delta_i} &= \frac{\delta\, u_k}{\delta\, \Delta_i} R_k + \frac{\delta\, R_k}{\delta\, \Delta_i} u_k \\ &= \frac{\delta\, u_k}{\delta\, u_{k-1}} \cdot \frac{\delta\, u_{k-1}}{\delta\, \Delta_i} \cdot R_k + \left(\frac{\delta\, R_k}{\delta\, u_{k-1}} \cdot \frac{\delta\, u_{k-1}}{\delta\, \Delta_i} + \frac{\delta\, R_k}{\delta\, R_{k-1}} \cdot \frac{\delta\, R_{k-1}}{\delta\, \Delta_i} \right) u_k\end{aligned}$$

with

$$\begin{aligned}\frac{\delta\, u_k}{\delta\, u_{k-1}} &= (1 - U) \exp(-\Delta_{k-1}/F)\ , \\ \frac{\delta\, R_k}{\delta\, u_{k-1}} &= -R_{k-1} \exp(-\Delta_{k-1}/D)\ , \qquad \text{and} \\ \frac{\delta\, R_k}{\delta\, R_{k-1}} &= (1 - u_{k-1}) \exp(-\Delta_{k-1}/D)\ .\end{aligned}$$

Hence,

$$\begin{aligned}\frac{\delta\, u_k}{\delta\, \Delta_i} &= \frac{\delta\, u_k}{\delta\, u_{k-1}} \cdot \frac{\delta\, u_{k-1}}{\delta\, \Delta_i} \qquad \text{and} \\ \frac{\delta\, R_k}{\delta\, \Delta_i} &= \frac{\delta\, R_k}{\delta\, u_{k-1}} \cdot \frac{\delta\, u_{k-1}}{\delta\, \Delta_i} + \frac{\delta\, R_k}{\delta\, R_{k-1}} \cdot \frac{\delta\, R_{k-1}}{\delta\, \Delta_i}\end{aligned}$$

can be calculated from $\frac{\delta\, u_{k-1}}{\delta\, \Delta_i}$ and $\frac{\delta\, R_{k-1}}{\delta\, \Delta_i}$. Hence, starting with the equations

$$\begin{aligned}\frac{\delta\, u_{i+1}}{\delta\, \Delta_i} &= -\frac{1}{F} u_i (1 - U) e^{-\Delta_i/F} = \frac{U - u_{i+1}}{F} \\ \frac{\delta\, R_{i+1}}{\delta\, \Delta_i} &= -\frac{1}{D} (R_i - u_i R_i - 1) e^{-\Delta_i/F} = \frac{1 - R_{i+1}}{D},\end{aligned}$$

the calculation of $\frac{\delta\, u_k R_k}{\delta\, \Delta_i}$ for $k > i$ is rather straightforward.

Acknowledgments

We thank Terry Sejnowski, Henry Markram, Misha Tsodyks, and Tony Zador for helpful and stimulating comments to our research. This work was supported by the Salk Sloan Foundation for Theoretical Neuroscience, project P12153 of the Fonds zur Förderung wissenschaftlicher Forschung (FWF), Austria, and the NeuroCOLT project of the EC (ESPRIT Working Group No. 27150).

References

Abbott, L. F., Varela, J. A., Sen, K. A., & Nelson, S. B. (1997). Synaptic depression and cortical gain control. *Science, 275*, 220–224.

Bertsekas, D. P. (1995). *Dynamic programming and optimal control* (Vol. 1). Belmont, MA: Athena Scientific.

Brumberg, J. C., Nowak, L. G., & McCormick, D. A. (2000). Ionic mechanisms underlying repetitive high frequency burst firing in supragranular cortical neurons. *Journal of Neuroscience, 20*(1), 4829–4843.

Dobrunz, L., & Stevens, C. F. (1999). Response of hippocampal synapses to natural stimulation patterns. *Neuron, 22*, 157–166.

Gray, C. M., & McCormick, D. A. (1996). Chattering cells: Superficial pyramidal neurons contributing to the generation of synchronous oscillations in the visual cortex. *Science, 274*, 109–113.

Gupta, A., Wang, Y., & Markram, H. (2000). Organizing principles for a diversity of GABAergic interneurons and synapses in the neocortex. *Science, 287*, 273–278.

Katz, B. (1966). *Nerve, muscle, and synapse*. New York: McGraw-Hill.

Magleby, K. (1987). Short term synaptic plasticity. In G. M. Edelman, W. E. Gall, & W. M. Cowan (Eds.), *Synaptic function*. New York: Wiley.

Markram, H., & Tsodyks, M. (1996). Redistribution of synaptic efficacy between neocortical pyramidal neurons. *Nature, 382*, 807–810.

Markram, H., Wang, Y., & Tsodyks, M. (1998). Differential signaling via the same axon of neocortical pyramidal neurons. *Proc. Natl. Acad. Sci., 95*, 5323–5328.

Powell, M. J. D. (1983). Variable metric methods for constrained optimization. In A. Bachem, M. Grotschel, & B. Korte (Eds.), *Mathematical programming: The state of the art* (pp. 288–311). Berlin: Springer-Verlag.

Steriade, M., Timofeev, I., Dürmüller, N., & Grenier, F. (1998). Dynamic properties of corticothalamic neurons and local cortical interneurons generating fast rhythmic (30–40 Hz) spike bursts. *Journal of Neurophysiology, 79*, 483–490.

Thomson, A. M. (1997). Activity-dependent properties of synaptic transmission at two classes of connections made by rat neocortical pyramidal axons in vitro. *J. Physiol., 502*, 131–147.

Varela, J. A., Sen, K., Gibson, J., Fost, J., Abbott, L. F., & Nelson, S. B. (1997). A quantitative description of short-term plasticity at excitatory synapses in layer 2/3 of rat primary visual cortex. *J. Neurosci, 17*, 220–224.

Wang, Z., & McCormick, D. A. (1993). Control of firing mode of corticotectal and corticopontine layer V burst generating neurons by norepinephrine. *Journal of Neuroscience, 13*(5), 2199–2216.

Received June 16, 2000; accepted January 23, 2001.